Published in final edited form as:
Cell Metab. 2012 December 5; 16(6): 777–788. doi:10.1016/j.cmet.2012.11.003.

Chronic Caloric Restriction Preserves Mitochondrial Function in Senescence Without Increasing Mitochondrial Biogenesis

Ian R. Lanza[1], **Piotrek Zabielski**[1], **Katherine A. Klaus**[1], **Dawn M. Morse**[1], **Carrie J. Heppelmann**[2], **H. Robert Bergen III**[2], **Surendra Dasari**[3], **Stephane Walrand**[1], **Kevin R. Short**[1], **Matthew L. Johnson**[1], **Matthew M. Robinson**[1], **Jill M. Schimke**[1], **Daniel R. Jakaitis**[1], **Yan W. Asmann**[3], **Zhifu Sun**[3], and **K. Sreekumaran Nair**[1,*]

[1]Division of Endocrinology and Metabolism, Mayo Clinic College of Medicine, 200 First St SW, Rochester, MN 55905

[2]Division of Biochemistry and Molecular Biology, Mayo Clinic College of Medicine, 200 First St SW, Rochester, MN 55905

[3]Division of Biomedical Statistics and Informatics, Mayo Clinic College of Medicine, 200 First St SW, Rochester, MN 55905

SUMMARY

Caloric restriction (CR) mitigates many detrimental effects of aging and prolongs lifespan. CR has been suggested to increase mitochondrial biogenesis, thereby attenuating age-related declines in mitochondrial function; a concept that is challenged by recent studies. Here we show that lifelong CR in mice prevents age-related loss of mitochondrial oxidative capacity and efficiency, measured in isolated mitochondria and permeabilized muscle fibers. We find that these beneficial effects of CR occur without increasing mitochondrial abundance. Whole-genome expression profiling and large-scale proteomic surveys revealed expression patterns inconsistent with increased mitochondrial biogenesis, which is further supported by lower mitochondrial protein synthesis with CR. We find that CR decreases oxidant emission, increases antioxidant scavenging, and minimizes oxidative damage to DNA and protein. These results demonstrate that CR preserves mitochondrial function by protecting the integrity and function of existing cellular components rather than by increasing mitochondrial biogenesis.

Keywords

Caloric Restriction; Calorie restriction; dietary restriction; aging; mitochondria; protein synthesis; skeletal muscle; mitochondrial biogenesis

*Corresponding author: K. Sreekumaran Nair, M.D., Ph.D. Professor of Medicine, Division of Endocrinology and Metabolism, Mayo Clinic College of Medicine, 200 First St SW, Rochester, MN 55905, Tel: 507-255-2415, nair@mayo.edu.

Accession Numbers

Complete microarray data have been deposited to Gene Expression Omnibus (GEO). The accession number for this dataset is GSE36285.

INTRODUCTION

Caloric restriction (CR) without malnutrition is widely studied for its influence on maximal lifespan and ability to delay the onset of many derangements related to old age (Weindruch and Walford, 1998). Experiments in yeast established a link between CR and mitochondria by showing CR increased mitochondrial respiration, and deleting the gene for cytochrome c abolished lifespan extension by CR (Lin et al., 2002). Subsequent studies in flies (Zid et al., 2009), mice (Nisoli et al., 2005), rats (Sreekumar et al., 2002), and humans (Civitarese et al., 2007) reported that CR increases mitochondrial DNA (mtDNA) abundance, protein expression, and gene transcripts involved in mitochondrial biogenesis. Furthermore, CR activated AMP kinase and Sirt1, both of which converge on PGC-1α to promote an oxidative phenotype in muscle (Haigis and Guarente, 2006). Such findings have spawned the widely accepted hypothesis that CR stimulates mitochondrial biogenesis.

CR has generated growing enthusiasm in the context of delaying mitochondrial aging. Specifically, mitochondrial capacity declines with aging (Short et al., 2005). The decline is linked to decreased mitochondria abundance (Conley et al., 2000), protein expression (Lanza et al., 2008), mRNA transcripts (Calleja et al., 1993), mtDNA (Short et al., 2005) and increased oxidative stress (Hepple et al., 2008; Michikawa et al., 1999). Furthermore, protein turnover, which maintains protein quality, appears to be reduced with aging (Henderson et al., 2009). Decreased ability to replace damaged proteins may explain why mitochondrial function decreases with aging, even after accounting for decreased mitochondrial content (Conley et al., 2000; Short et al., 2005).

In several instances, CR has been shown to preserve mitochondrial function in aging rodents (Desai et al., 1996; Hepple et al., 2005; Zangarelli et al., 2006), but new reports question if CR truly increases mitochondrial biogenesis (Hancock et al., 2011; Miller et al., 2011). Hancock *et al.* could not reproduce the work of Nisoli *et al.* (Nisoli et al., 2005), who reported increased mitochondrial proteins, DNA, and mRNA abundance in response to 30% CR in mice. Hancock *et al.* propose that CR protects mitochondria with aging, not by stimulating mitochondrial biogenesis, but by protecting against DNA damage, enzyme abnormalities, and loss of mitochondria. In support, others demonstrated that CR increases PGC-1α mRNA, but there was no increase in PGC-1α protein expression or mitochondrial protein synthesis (Miller et al., 2011). Furthermore, food restricted animals (Giroud et al., 2010) and humans (Henderson et al., 2010) exhibit protein-sparing strategies such as decreased synthesis and breakdown of proteins. These recent studies challenge the idea that CR increases mitochondrial biogenesis and question the teleological sense of upregulating an energetically expensive process (i.e., protein synthesis) during energy deprivation.

Here, we employed several methodologies to evaluate skeletal muscle mitochondrial physiology, abundance, transcriptome, proteome, protein synthesis and post-translational modification of proteins in the context of CR and aging in mice. Our data show that CR preserves mitochondrial capacity and efficiency in aging mice without increasing mitochondrial biogenesis. We find that CR does not stimulate the synthesis of new mitochondrial proteins, but rather minimizes damage to existing cellular components through decreased mitochondrial oxidant emission and up-regulated antioxidant defenses.

RESULTS

CR prevents age-related decline in mitochondrial respiratory function

Mitochondrial function was assessed in permeabilized fibers and isolated mitochondria from gastrocnemius muscle. In isolated mitochondria, state 3 respiration was reduced with age in *ad libitum* fed mice, expressed per tissue wet weight (Figure 1A). The age-related decline

was attenuated by CR (Figure 1A). We removed the influence of mitochondrial content by expressing respiration rates relative to mitochondrial protein (figure 1B) and mitochondrial DNA copy (Figure 1C). This eliminated the age-associated reduction in respiratory function and suggests that mitochondrial content is a major determinant of age-related reductions in oxidative capacity. However, OCR mice exhibited elevated respiratory function compared to OAL when normalized for mitochondrial content (Figures 1B, 1C). In permeabilized fibers, state 3 through complex I was significantly reduced with age with similar trends for complex I+II and complex II (Figure 1D). As with isolated mitochondria, the increased respiratory function in permeabilized fibers of OCR animals persisted after normalizing to mtDNA (Figure 1E). Citrate synthase activity was measured in a subset of mice in quadriceps, gastrocnemius, heart, and liver (Figure S1). A similar pattern of increased mitochondrial function by CR was observed in these tissues except heart, which showed no change in citrate synthase activity with aging or CR (Figure S1).

Mitochondrial efficiency, evaluated by the respiratory control ratio (RCR, state 3/state 4), was lower in OAL compared to YAL, indicating increased proton leak with age (Figure 1F). This uncoupling was attenuated by CR. Furthermore, phosphorylation efficiency (ADP:O) was significantly decreased with age in AL but not CR mice (Figure 1G). Together, these data show that CR prevents age-related decreases in mitochondrial efficiency.

CR does not prevent age-related reduction in mitochondrial content of skeletal muscle

Since we found that CR preserved mitochondrial function, we determined the influence of CR on mitochondrial abundance. Electron microscopy revealed that average organelle perimeter, height, and area were lower in OAL than YAL, but similar in YAL and OCR (Figure 2D). Mitochondrial density by area was lower in old mice, regardless of diet (Figure 2E). The decline in mitochondrial density in spite of preserved mitochondrial size with CR can be explained by a non-significant trend for reduced mitochondrial number with CR (Figure 2F). Consistent with the electron microscopy findings, CR did not prevent the age-related reduction in mtDNA abundance (Figure 2G). CR did not prevent the decline in mtDNA abundance in quadriceps or heart muscles, yet mtDNA was notably elevated in liver of CR mice (Figure S2). Immunoblots for respiratory chain complexes I, II, III, IV, and V revealed that CR did not prevent the age-related decrease in mitochondrial protein expression (Figure 2H). Altogether, these data indicate that chronic CR does not prevent the reduction in mitochondrial abundance with old age in skeletal muscle.

Transcriptome analyses do not indicate up-regulated mitochondrial biogenesis in CR

We performed skeletal muscle whole-genome transcript profiling to determine if CR induced a gene expression profile consistent with increased mitochondrial biogenesis. There were 3,187 genes for which expression values differed significantly between OAL and YAL (Figure 3A). Of these genes, 130 were mitochondrial, of which 87 were upregulated and 43 were down-regulated in OAL vs. YAL. Thirty-three of these genes encoded tricarboxylic acid (TCA) cycle and oxidative phosphorylation proteins, of which 26 were up-regulated and 7 down-regulated in OAL vs. YAL (Figure 3A, table S1). We also identified 26 genes that are involved in transcription and translation of mitochondrial proteins and found that 21 genes were significantly up-regulated in OAL vs. YAL. Next, we used Ingenuity Pathway Analysis (IPA), focusing on cellular energy metabolism, oxidative stress, and protein turnover pathways. Aging was associated with gene expression patterns consistent with up-regulation of pyruvate metabolism, oxidative phosphorylation, protein synthesis and degradation, and cellular response to oxidative stress (Figure 3C). The specific molecules included in each pathway and a complete list of altered canonical pathways are given in Table S2.

Comparing OCR vs. OAL revealed 1,236 genes that were differentially expressed between the groups, of which 73 were mitochondrial (Figure 3B, Table S3). Of these genes, 24 were up-regulated and 49 were down-regulated in OCR vs. OAL. Ten genes were mitochondrial, with 4 up-regulated and 6 down-regulated in OCR vs. OAL. There were 24 genes involved in mitochondrial transcription and translation. Twenty of these genes were down-regulated in OCR compared to OAL. Ingenuity Pathway Analysis (Figure 3D) did not detect any significant changes in pathways involving TCA cycle, oxidative phosphorylation, glycolysis, or pyruvate metabolism. Pathways that were significantly up-regulated in OCR vs. OAL included protein degradation, glutathione metabolism and Nrf2-mediated response to oxidative stress. The majority of genes involved in the protein synthesis pathway were down-regulated in OCR vs. OAL (Figure 3D). The specific genes included in each pathway and a complete list of altered canonical pathways are given in Table S4. In sum, we find that the transcriptional signals involved in mitochondrial energy metabolism and protein synthesis are elevated with aging, and chronic CR does not influence these transcriptional signals.

Quantitative proteomics reveals down-regulation of mitochondrial pathways with CR

We completed a large-scale proteomic survey to complement the microarray data since genes are ultimately expressed as proteins and there is potential inequality between gene expression and protein abundance (Mootha et al., 2003). We performed stable isotope labeling of whole animals (SILAC mouse) followed by mass spectrometry-based quantitative proteomics to measure the relative abundance of individual skeletal muscle proteins (Walther and Mann, 2011). Individual peptides corresponding to 595 proteins were quantified by mass spectrometry. Of these proteins, 178 were mitochondrial-related, with 104 up-regulated and 74 down-regulated in OAL vs. YAL (figure 4A, Table S5). 84 of these proteins were directly related to TCA cycle and oxidative phosphorylation, of which 53 were increased and 31 decreased in OAL vs. YAL. Pathway analyses revealed clear, significant up-regulation of the citrate cycle and protein synthesis, but down-regulation of glycolysis and pyruvate metabolism in OAL vs. YAL (Figure 4C). The specific molecules included in each pathway as well as a complete list of altered canonical pathways are given in Table S6.

In the OCR vs. OAL comparison, 179 mitochondrial proteins were identified and quantified, of which 49 were up-regulated and 130 down-regulated in OCR vs. OAL (Figure 4B, Table S7). Of the 87 proteins directly involved in the TCA cycle and oxidative phosphorylation, 22 were significantly increased in OCR vs. OAL while the other 65 proteins were significantly decreased in OCR vs. OAL (Figure 4B). Pathway analysis revealed that all mitochondrial-related pathways (i.e., citrate cycle, oxidative phosphorylation, pyruvate metabolism) were down-regulated with CR, as was protein synthesis (Figure 4D). Notably, the glycolysis pathway was strongly upregulated with CR, which may reflect increase flux through aerobic glycolysis as a carbon source for the tricarboxylic acid cycle. We also cannot ignore the possibility that CR may also increase glycogen synthesis from lactate given the observed increases in lactate dehydrogenase A, fructose-1,6-bisphosphatase, and phosphoglucomutase with CR (table S8). The specific molecules included in each pathway as well as a complete list of altered canonical pathways are given in Table S8. Based on this large-scale quantitative proteomic approach, we show that long-term CR does not stimulate mitochondrial biogenesis in spite of the observation that CR enhances mitochondrial function.

CR decreases *in vivo* synthesis of skeletal muscle proteins

To further investigate the influence of CR on mitochondrial biogenesis, we measured the fractional synthesis rates (FSR) of individual skeletal muscle proteins, including ATP

synthase. Animals were injected with [ring-$^{13}C_6$]phenylalanine, and the incorporation of the isotope tracer into skeletal muscle proteins was measured by mass spectrometry. Mixed muscle protein (MMP) synthesis was similar in YAL and OAL, but significantly lower in OCR, indicating that overall protein synthesis decreased with CR (Figure 5B). We found a similar pattern in a variety of tissues (gastrocnemius, quadriceps, tibialis anterior, heart, and liver) in a subset of mice (Figure S3A–E). Since MMP synthesis represents the average FSR of many individual proteins that may respond to CR in different directions, we also measured FSR of individual mitochondrial and contractile proteins separated by 2D electrophoresis (Figure 5A). A representative mitochondrial protein, ATP synthase β, showed a decline with age in *ad libitum* fed animals, but a further decline with CR (Figure 5B). Synthesis rates of individual contractile proteins were also significantly lower in OCR (Figure 5B). In a subset analysis, mitochondrial protein FSR was lower in OCR compared with OAL mice in quadriceps, tibialis anterior, heart, and liver (Figure S3F–J). These data show that CR decreases synthesis rates of mitochondrial proteins.

CR decreases cellular oxidative damage by decreasing skeletal muscle oxidant emission and increasing oxidant scavenging

In the absence of increased mitochondrial biogenesis with CR, we evaluated mechanisms to explain the protective effects of CR on mitochondrial physiology. We first assessed protein quality through an unrestricted evaluation of post-translational modifications in the proteomics database. We found that oxidation and deamidation were the most abundant modifications detected in the samples (Table 1). Pair-wise comparison of oxidative modification abundances showed that OCR group had lower oxidation levels compared to OAL and YAL (Table 1). Also, OCR and YAL mice had similar deamidation and were much lower than OAL (Table 1). We detected a total of seven previously uncharacterized PTMs on cysteine, methionine, and tryptophan residues, which are considered prime substrates for ROS (Table 1). The abundance of semitryptic peptides was used as a qualitative index of *in vivo* proteolytic damage. OCR mice had the lowest abundance of semitryptic peptides (2.48%) compared to that of OAL (2.71%) and YAL (2.77%). We also measured DNA oxidative damage from abundance of the oxidized derivative of deoxyguanosine, 8-oxo-2′-deoxyguanosine (8-oxo-dG). We found that OCR mice exhibited lower 8-oxo-dG levels compared to OAL mice (Figure 6A), indicating that CR prevents the age-related increase in DNA damage. To evaluate potential mechanisms to explain why CR attenuates oxidative damage, we measured hydrogen peroxide (H_2O_2) production in permeabilized muscle fibers. The rate of H_2O_2 emission increased with age, but was prevented by CR (Figure 6D), indicating that CR protects against the rise in oxidant production with aging. We also measured the activity of 2 enzymes involved in scavenging reactive oxygen species in skeletal muscle. Although total superoxide dismutase (SOD) activity was unchanged with aging or CR (Figure 6G), we found that catalase activity was significantly elevated in CR (Figure 6H). These data show that CR attenuates age-related cellular oxidative damage, decreases mitochondrial oxidant emission, and increases the activity of endogenous antioxidants. Such effects likely contribute to the preservation of mitochondrial function with CR in the absence of increased mitochondrial biogenesis.

DISCUSSION

This study shows that chronic caloric restriction preserves mitochondrial function in aging skeletal muscle. However, CR did not prevent the decline in mitochondrial abundance with aging; a finding that is inconsistent with the notion that CR increases mitochondrial biogenesis. Using complementary information from whole-genome expression, large-scale proteomic surveys, and protein synthesis rates, we find no evidence that CR increases mitochondrial biogenesis. Chronic CR appears to preserve mitochondrial function by

maintaining the integrity of protein and DNA by decreasing mitochondrial oxidant emission and increasing endogenous antioxidant activity.

Numerous studies suggest that CR attenuates the age-related decline mitochondrial function (Desai et al., 1996; Hepple et al., 2006; Zangarelli et al., 2006). The current study evaluated mitochondrial function in isolated organelles and permeabilized fibers. Although a recent report indicates that age-related functional impairments are less evident in permeabilized fibers compared with isolated mitochondria (Picard et al., 2010), we reached similar conclusions from both methods; specifically, that age-related declines in mitochondrial capacity are attenuated by caloric restriction. In terms of bioenergetic efficiency, some investigators proposed that CR increases mitochondrial proton leak (Lambert and Merry, 2004), while others find that CR decreases proton leak (Zangarelli et al., 2006). The current data are consistent with the latter, showing that CR is able to prevent the age-related decline in coupling efficiency. A lingering question is whether CR increases mitochondrial abundance. Although CR increased mitochondrial mass in cultured HeLa cells and rat liver (Lopez-Lluch et al., 2006), data from skeletal muscle show no change in mitochondrial protein expression with CR (Hancock et al., 2011). Here we employed multiple independent measurements to demonstrate that chronic CR does not prevent the loss of mitochondrial abundance with aging in spite of preserving mitochondrial function. When mitochondrial respiration rates were expressed relative to mitochondrial mass (i.e., protein content or mtDNA), we found that respiration rates were elevated in older CR animals, indicating that CR increases the intrinsic function of the respiratory chain machinery.

The prevailing hypothesis that CR increases mitochondrial biogenesis is supported by reports that CR increases mitochondrial gene transcripts (Baker et al., 2006; Civitarese et al., 2007; Sreekumar et al., 2002). These studies provide knowledge of transcriptional regulation of mitochondrial biogenesis, but should be cautiously interpreted since mRNA abundance and protein expression are not always equal. Here we combined large-scale quantitative proteomics with RNA expression profiles to provide insight into the mechanisms by which CR attenuates mitochondrial aging. Most mitochondrial genes were downregulated with CR, consistent with the transcriptional profile of adult Rhesus monkeys that were caloric restricted for 9 years (Kayo et al., 2001). Others report transcriptional changes in skeletal muscle consistent with increased protein synthesis with CR (Weindruch et al., 2001). We also found that CR induced a gene expression pattern consistent with increased protein turnover, however CR also demonstrated a transcriptional pattern consistent with decreased transcription and translation of mitochondrial proteins. Furthermore, the proteomic survey in CR animals revealed a clear decrease in the abundance of mitochondrial proteins compared with *ad libitum* fed old mice. A discordance between mRNA and protein expression was evident from a comparison of fold-changes in mitochondrial targets that were common to microarray and SILAC proteomics (Figure S4); a finding that underscores the importance of considering transcriptional and posttranscriptional mechanisms that may be influenced by CR.

We used *in vivo* labeling of muscle proteins to determine if CR reduced translation of transcripts to protein. Several reports indicate that CR increases protein synthesis at the whole-body level (Lewis et al., 1985), liver (Merry et al., 1987), muscle (el Haj et al., 1986), and mitochondria (Zangarelli et al., 2006), while others report that CR does not increase mitochondrial protein synthesis (Miller et al., 2011). Here we found lower protein synthesis with CR. Although our data indicate that, in general, protein synthesis decreases with CR, it is important to highlight that mixed muscle FSR represents an average FSR of many proteins, some of which decrease with CR while others may increase. In consideration of this issue, we demonstrate that CR decreases FSR of individual skeletal muscle proteins. These findings argue against the hypothesis that CR increases mitochondrial biogenesis.

If CR does not increase mitochondrial biogenesis, then to what can we attribute the robust preservation of mitochondrial function? Our data suggest that CR attenuates oxidative damage by decreasing ROS emission and increasing endogenous antioxidant activity. Previous data indicated that CR reduces mitochondrial ROS emission (Lambert and Merry, 2004), which we demonstrate here in permeabilized muscle fibers. The activity of antioxidant enzymes has been reported to decrease (Luhtala et al., 1994) or remain unchanged (Sohal et al., 1994) with CR. Similarly, SOD activity is unchanged by CR yet CR increased catalase activity. Decreased ROS production and increased antioxidant defense is consistent with CR decreasing oxidative damage to tissues (Sohal and Weindruch, 1996), thereby preserving the function of cells and cellular components such as mitochondria.

Accordingly, we find decreased deamidation and oxidation in skeletal muscle from CR mice and fewer semi-tryptic peptides. Also, 8-oxo-dG, a marker of oxidative damage to DNA, was lower in skeletal muscle from CR compared to *ad libitum* fed mice. The role of CR in augmenting the capacity of endogenous antioxidant defenses in skeletal muscle is a likely mechanism by which CR decreases oxidative stress. Alternatively, CR may attenuate oxidative damage through increased protein degradation either through autophagy or the ubiquitin-proteasome system. Indeed, CR induces autophagy in many tissues, including heart (Han et al., 2012; Wohlgemuth et al., 2007), liver (Donati et al., 2001; Wohlgemuth et al., 2007), kidney (Kume et al., 2010), nematodes and cancer cells (Morselli et al., 2010). The few studies that have focused on skeletal muscle showed that CR optimized the proteasome pathway (Hepple et al., 2008) suggesting that CR may increase protein degradation. However, contrasting data come from studies showing that chronic CR activated protein-sparing strategies such as decreased urinary nitrogen loss (Cahill, 1970; Cahill et al., 1966) and decreased protein turnover (Nair et al., 1989). Short-term caloric restriction in humans also reduces protein turnover (Gallagher et al., 2000; Henderson et al., 2010). Furthermore, CR reduces the mRNA levels of proteasome subunits involved in protein degradation (Sreekumar et al., 2002). While induction of autophagy remains a plausible mechanism by which chronic CR minimizes accumulation of damaged cellular components, the current study highlights the important role of ROS emission and oxidant scavenging reactions with chronic CR.

In conclusion, life-long CR in mice enhances skeletal muscle mitochondrial oxidative capacity by increasing the intrinsic function and efficiency of mitochondrial machinery. We propose that maintenance of highly functional mitochondria by CR is not the result of increased mitochondrial biogenesis, but results from attenuated mitochondrial oxidant emission, increased oxidant scavenging, and decreased cellular oxidative damage; all of which could be expected to contribute to the maintenance of the functional integrity of the mitochondrial machinery in the absence of any evidence for increased synthesis of mitochondrial proteins.

EXPERIMENTAL PROCEDURES

Animals

The Mayo Institutional Animal Care and Use Committee approved the protocol. Mice (male B6D2F1) were obtained from the National Institute on Aging Caloric Restricted Colony. Young mice (8 mo) were given chow (NIH31/NIA) and water *ad libitum*. Old mice (24 mo) were either fed ad libitum or caloric restricted by 40%. After 10 days of acclimation, body composition was measured by Echo-MRI (Echo Medical Systems, Houston, TX). Mice were sacrificed by CO_2, and a portion of the gastrocnemius was placed on ice for fresh tissue assays. The contralateral medial gastrocnemius and other tissues were immediately frozen in liquid nitrogen and stored at −80°C.

Respiration of isolated mitochondria and permeabilized muscle fibers

Mitochondria were isolated by differential centrifugation, as previously described (Lanza and Nair, 2009). Respiration was measured in duplicate (Oxygraph, Oroboros Instruments, Innsbruck, Austria) using a stepwise protocol to assess states 1, 2, 3, 4 with electron flow through various respiratory chain complexes (Gnaiger, 2009). Oxygen flux rates were expressed per tissue wet weight, per mg mitochondrial protein (Bio-Rad DC Protein Assay, Bio-Rad, Hercules, CA), and per mtDNA copy number. The respiratory control ratio was calculated as the quotient of state 3 and state 4 respiration rates.

Respiration studies were also conducted in permeabilized muscle fibers as described previously (Anderson et al., 2009; Hutter et al., 2007). Fiber bundles (~5mg) were permeabilized by saponin (50μg/ml) and washed in buffer containing (in mM) 110 K-MES, 35 KCl, 1 EGTA, 5 K_2HPO_4, 3 $MgCl_2$-$6H_2O$, 0.05 pyruvate, and 0.02 malate, and 5 mg/ml BSA (pH 7.4, 295 mOsm) (Anderson et al., 2009). Respiration was measured with 50μM benzyltoluene sulfonamide to inhibit fiber contraction (Anderson et al., 2009). All respiration measurements in permeabilized fibers were performed between 200–400μM oxygen and expressed per tissue wet weight.

Electron microscopy

A portion of the gastrocnemius was fixed (30% formaldehyde, 10% glutaraldehyde), stained with uranyl acetate and embedded in epoxy resin. Sections stained with lead citrate were examined by a transmission electron microscope (JEOL ExII, Peabody, MA) at 25,000X magnification by a blinded investigator. Ten digital images per sample were analyzed using NIH Image J software for measurement of mitochondrial area and perimeter. Mitochondrial density by area was computed as the total area (μm^2) of mitochondria divided by the area of the field of view, calibrated to a digital scale bar.

Mitochondrial DNA (mtDNA) copy number

DNA was extracted from frozen tissues using a QIAamp DNA mini kit (Qiagen, Valencia, CA). Relative mtDNA copy numbers were determined by real-time PCR (Applied Biosystems 7900HT Sequence Detection System) using primer/probe sets targeted to mtDNA-encoded NADH dehydrogenase subunits 1 (ND1) and 4 (ND4). Samples were run in duplicate and normalized for the nuclear housekeeping gene 28S ribosomal DNA.

Protein expression by SILAC mouse

We used quadriceps muscle tissue from fully labeled ($^{13}C_6$-lysine) mice (SILAC mice) combined with mass spectrometry to compare the relative expression of proteins in YAL, OAL and OCR mice (n=3 per group). Tissues were pulverized and sonicated in RIPA buffer. Samples were prepared for SDS-PAGE at final protein concentration of 1μg/μl. Lysates from experimental animals were mixed in 1:1 (protein/protein) ratio with lysate obtained from SILAC mouse. 15μg/well of combined protein samples were resolved on 4–12% NuPAGE Novex Bis-Tris Midi gels. Following in-gel trypsin digestion, individual peptides were identified and quantified by nanoLC-LTQ-ORBITRAP (LC-MS/MS). Relative expression of skeletal muscle proteins was determined using Rosetta Elucidator software (Seattle, WA).

Gene expression analysis

Total RNA was extracted from tissue (Qiagen RNeasy Fibrous Tissue Kit, Qiagen, Valencia, CA), and the gene expression microarray was carried out by the Advanced Genomics Technology Center at Mayo using Illumina MouseWG-6 v2.0 BeadChip. The probe level raw data were normalized using the quantile method implemented in GenomeStudio

(v2011). No batch effects were observed between chips. The technical replicates between chips had high correlation (R^2>0.99). The probes with detection p value greater than 0.05 across all samples were filtered which resulted in 22,611 probes kept in final analyses. Expression data for the replicates were averaged. The ANOVA model compared differentially expressed genes with batches of chips and sample locations on each chip as covariates. Pair-wise comparisons were conducted for differentially expressed genes between groups. Probes with $p<0.05$ were claimed to be significant.

Protein synthesis rates

Protein synthesis rates of mixed muscle proteins and several individual muscle proteins were measured in rats as described previously (Jaleel et al., 2008). Rats were used because of large tissue requirements. Young (7 months) and old (27 months) rats (F344xBN F1 hybrids) were provided with *ad libitum* access to food and water. The OCR group received 60% of the *ad libitum* intake starting at 4 months of age. Following tail vein injection of [$^{13}C_6$]phe (Cambridge Isotope Laboratories, Cambridge, MA; 99 atom percent excess, 15mg/kg), rats were anesthetized with pentobarbital (50 mg/kg) and quadriceps muscle was removed and frozen. Frozen samples were homogenized in 35 mM Tris, 9 M urea, 4% CHAPS, 65 mM DTT. Equal amounts of protein were used to rehydrate 24-cm, pH 4–7, immobilized pH gradient strips (Bio-Rad Laboratories, Hercules, CA) and isoelectric focusing was performed in a Protean IEF Cell (Bio-Rad) using parameters described previously (Jaleel et al., 2008). Separation by molecular weight (2^{nd} dimension) was accomplished by vertical 12%, 24 × 20-cm dimension SDS-PAGE (Ettan DALT system; GE Healthcare Bio-Sciences, Piscataway, NJ). Silver stained protein gel spots were previously identified in rat skeletal muscle by liquid chromatography-tandem mass spectrometry (Jaleel et al., 2008). Gels were run in duplicate and protein gel spots corresponding to ATP synthase β, actin, myosin light chain 1, and myosin light chain 2 were excised. Gel spots were hydrolyzed and the amino acid residues were derivatized to their N-heptafluorobutyryl methyl esters and the ^{13}C enrichment of [ring-$^{13}C_6$]phe was measured by MS/MS, as described previously (Jaleel et al., 2008). Tissue fluid enrichment was used as the precursor pool for FSR calculations. Sulfosalycilic acid was used to extract tissue fluid amino acids and analyzed as their t-butyldimethylsilyl ester derivative for measurement of molar percent excess of $^{13}C_6$-phe. Fractional synthesis rates were calculated as (Jaleel et al., 2008).

Additional protein synthesis measurements were performed in a subset of mice (N=6 per group) to evaluate MMP synthesis and FSR of mitochondrial proteins in multiple tissues. Mice were given a flooding dose (15mg/kg) of [ring-$^{13}C_6$]phe, and skeletal muscles, heart, and liver were removed under anesthesia and frozen in liquid nitrogen. Mitochondria were isolated from frozen tissues, isotopic enrichment was measured by mass spectrometry, and protein synthesis rates were calculated as described above.

Posttranslational modification (PTM) detection and quantification

We followed a two-step workflow to detect and quantify unanticipated PTMs from MS/MS data of each mice cohort. In the first step, MS/MS were identified with a regular MyriMatch (Tabb et al., 2007) database search configured to derive semitryptic peptides from the RefSeq protein sequence database (version 53) while looking for sample handling modifications. IDPicker (Ma et al., 2009) filtered the results at 2% False Discovery Rate (FDR) using a target-decoy search paradigm. Proteins with at least two confident peptide identifications were added to a subset database. In the second step, DirecTag-TagRecon software used the subset proteins to search for unexpected PTMs in the data set. DirecTag (Tabb et al., 2008) generated best 50 sequence tags for each MS/MS, which were reconciled against the subset database by TagRecon (Dasari et al., 2010) while making allowances for unanticipated mass shifts in peptides. Peptide identifications were filtered by IDPicker at 2%

FDR, and PTMDigger applied a series of stringent filtering criteria to remove peptides with spurious modifications (Dasari et al., 2011).

Hydrogen peroxide emission

An adaptation of the methodology developed by Anderson et al. (Anderson et al., 2009) was used to measure H_2O_2 emission in permeabilized muscle fibers. Duplicate sets of permeabilized muscle fibers were prepared as described above but with preincubation in 10mM pyrophosphate to deplete endogenous adenylates (Anderson et al., 2009). A Fluorolog 3 (Horiba Jobin Yvon) spectrofluorometer was used to monitor Amplex Red (Invitrogen) oxidation in fibers. Fiber bundles were placed in a quartz cuvette with 2ml buffer z containing 2μg/ml oligomycin. Glutamate (5μM), malate (2μM), and succinate (0.75mM) were added to stimulate H_2O_2 production under state 4 conditions. The fluorescent signal was corrected for background autooxidation and calibrated to a standard curve. H_2O_2 production rates were expressed per tissue wet weight.

DNA Oxidation

We measured the DNA adduct biomarker of oxidative stress, 8-oxo-dG, by LC/MS/MS as described previously (Short et al., 2005). Briefly, DNA was isolated using Sodium Iodide (DNA Extractor TIS Kit, Wako Richmond, VA). A known amount of internal standard solution was added to the DNA samples prior to hydrolysis as instructed in the 8-OHdG Assay Preparation Reagent Set from Wako Chemicals (Richmond, VA). A seven point concentration curve was simultaneously made for 2′-deoxyguanosine (dG) and 8-hydroxy-2′-deoxyguanosine (8-OHdG) by adding the same amount of internal standard solution to each point. All standards and hydrolyzed samples were measured by LC/MS/MS. Briefly, dG and 8-OHdG were separated on a Waters C18 BEH 2.1×50mm column at 0.4 ml/min flow rate via Waters Acquity UPLC system (Milford, MA). All ions were run in negative electrospray ionization using selected-reaction-monitoring (SRM) for transitions on a TSQ Quantum Ultra from Thermo Scientific (Waltham, MA).

Antioxidant enzyme activities

Muscle total superoxide dismutase activity was measured in muscle lysate as the consumption of xanthine oxidase generated superoxide radical by SOD in a competitive reaction with a tetrazolium salt (Cayman Chemical Company, Ann Arbor, MI). Catalase activity was determined in muscle lysate spectrophotometrically by measuring peroxide removal. This is a direct kinetic assay that follows the action of catalase on hydrogen peroxide and is based upon measurement of the ultraviolet absorption of peroxide at 240 nm every 30 seconds for 2 minutes.

Statistical analyses

Data are presented as mean±SEM. All variables were analyzed by analysis of variance with group (YAL, OAL, OCR) as the main effect. When significant ($p<0.05$) main effect was found, Tukey's HSD procedure was used for pairwise comparisons across groups while maintaining 5% type I error rate.

Supplementary Material

Refer to Web version on PubMed Central for supplementary material.

Acknowledgments

We thank Mai Persson, Charles Ford, Jaime Gransee, and Melissa Aakre for technical expertise. We are grateful to Drs. Ethan Anderson and Darryl Neufer for guidance on H_2O_2 production measurements. Support was provided by

National Institute on Aging Grant RO1-AG09531, the Mayo Foundation, the Dole-Murdock Professorship (K. S. Nair), T32 DK007198 and KL2TR000136-07 (I.R. Lanza), and the American Federation for Aging Research (K.R. Short).

References

Anderson EJ, Lustig ME, Boyle KE, Woodlief TL, Kane DA, Lin CT, Price JW 3rd, Kang L, Rabinovitch PS, Szeto HH, et al. Mitochondrial H2O2 emission and cellular redox state link excess fat intake to insulin resistance in both rodents and humans. J Clin Invest. 2009; 119:573–581. [PubMed: 19188683]

Baker DJ, Betik AC, Krause DJ, Hepple RT. No decline in skeletal muscle oxidative capacity with aging in long-term calorically restricted rats: effects are independent of mitochondrial DNA integrity. J Gerontol A Biol Sci Med Sci. 2006; 61:675–684. [PubMed: 16870628]

Cahill GF Jr. Starvation in man. N Engl J Med. 1970; 282:668–675. [PubMed: 4915800]

Cahill GF Jr, Herrera MG, Morgan AP, Soeldner JS, Steinke J, Levy PL, Reichard GA Jr, Kipnis DM. Hormone-fuel interrelationships during fasting. J Clin Invest. 1966; 45:1751–1769. [PubMed: 5926444]

Calleja M, Pena P, Ugalde C, Ferreiro C, Marco R, Garesse R. Mitochondrial DNA remains intact during Drosophila aging, but the levels of mitochondrial transcripts are significantly reduced. J Biol Chem. 1993; 268:18891–18897. [PubMed: 8395521]

Civitarese AE, Carling S, Heilbronn LK, Hulver MH, Ukropcova B, Deutsch WA, Smith SR, Ravussin E. Calorie restriction increases muscle mitochondrial biogenesis in healthy humans. PLoS Med. 2007; 4:e76. [PubMed: 17341128]

Conley KE, Jubrias SA, Esselman PC. Oxidative capacity and ageing in human muscle. J Physiol. 2000; 526(Pt 1):203–210. [PubMed: 10878112]

Dasari S, Chambers MC, Codreanu SG, Liebler DC, Collins BC, Pennington SR, Gallagher WM, Tabb DL. Sequence tagging reveals unexpected modifications in toxicoproteomics. Chem Res Toxicol. 2011; 24:204–216. [PubMed: 21214251]

Dasari S, Chambers MC, Slebos RJ, Zimmerman LJ, Ham AJ, Tabb DL. TagRecon: high-throughput mutation identification through sequence tagging. J Proteome Res. 2010; 9:1716–1726. [PubMed: 20131910]

Desai VG, Weindruch R, Hart RW, Feuers RJ. Influences of age and dietary restriction on gastrocnemius electron transport system activities in mice. Arch Biochem Biophys. 1996; 333:145–151. [PubMed: 8806765]

Donati A, Cavallini G, Paradiso C, Vittorini S, Pollera M, Gori Z, Bergamini E. Age-related changes in the autophagic proteolysis of rat isolated liver cells: effects of antiaging dietary restrictions. J Gerontol A Biol Sci Med Sci. 2001; 56:B375–383. [PubMed: 11524438]

el Haj AJ, Lewis SE, Goldspink DF, Merry BJ, Holehan AM. The effect of chronic and acute dietary restriction on the growth and protein turnover of fast and slow types of rat skeletal muscle. Comp Biochem Physiol A Comp Physiol. 1986; 85:281–287. [PubMed: 2876836]

Gallagher D, Kovera AJ, Clay-Williams G, Agin D, Leone P, Albu J, Matthews DE, Heymsfield SB. Weight loss in postmenopausal obesity: no adverse alterations in body composition and protein metabolism. Am J Physiol Endocrinol Metab. 2000; 279:E124–131. [PubMed: 10893331]

Giroud S, Perret M, Stein P, Goudable J, Aujard F, Gilbert C, Robin JP, Le Maho Y, Zahariev A, Blanc S, et al. The grey mouse lemur uses season-dependent fat or protein sparing strategies to face chronic food restriction. PLoS One. 2010; 5:e8823. [PubMed: 20098678]

Gnaiger E. Capacity of oxidative phosphorylation in human skeletal muscle: new perspectives of mitochondrial physiology. Int J Biochem Cell Biol. 2009; 41:1837–1845. [PubMed: 19467914]

Haigis MC, Guarente LP. Mammalian sirtuins--emerging roles in physiology, aging, and calorie restriction. Genes Dev. 2006; 20:2913–2921. [PubMed: 17079682]

Han X, Turdi S, Hu N, Guo R, Zhang Y, Ren J. Influence of long-term caloric restriction on myocardial and cardiomyocyte contractile function and autophagy in mice. J Nutr Biochem. 2012

Hancock CR, Han DH, Higashida K, Kim SH, Holloszy JO. Does calorie restriction induce mitochondrial biogenesis? A reevaluation. FASEB J. 2011; 25:785–791. [PubMed: 21048043]

Henderson GC, Dhatariya K, Ford GC, Klaus KA, Basu R, Rizza RA, Jensen MD, Khosla S, O'Brien P, Nair KS. Higher muscle protein synthesis in women than men across the lifespan, and failure of androgen administration to amend age-related decrements. FASEB J. 2009; 23:631–641. [PubMed: 18827019]

Henderson GC, Nadeau D, Horton ES, Nair KS. Effects of adiposity and 30 days of caloric restriction upon protein metabolism in moderately vs. severely obese women. Obesity (Silver Spring). 2010; 18:1135–1142. [PubMed: 20134416]

Hepple RT, Baker DJ, Kaczor JJ, Krause DJ. Long-term caloric restriction abrogates the age-related decline in skeletal muscle aerobic function. FASEB J. 2005; 19:1320–1322. [PubMed: 15955841]

Hepple RT, Baker DJ, McConkey M, Murynka T, Norris R. Caloric restriction protects mitochondrial function with aging in skeletal and cardiac muscles. Rejuvenation Res. 2006; 9:219–222. [PubMed: 16706647]

Hepple RT, Qin M, Nakamoto H, Goto S. Caloric restriction optimizes the proteasome pathway with aging in rat plantaris muscle: implications for sarcopenia. Am J Physiol Regul Integr Comp Physiol. 2008; 295:R1231–1237. [PubMed: 18703409]

Hutter E, Skovbro M, Lener B, Prats C, Rabol R, Dela F, Jansen-Durr P. Oxidative stress and mitochondrial impairment can be separated from lipofuscin accumulation in aged human skeletal muscle. Aging Cell. 2007; 6:245–256. [PubMed: 17376148]

Jaleel A, Short KR, Asmann YW, Klaus KA, Morse DM, Ford GC, Nair KS. In vivo measurement of synthesis rate of individual skeletal muscle mitochondrial proteins. Am J Physiol Endocrinol Metab. 2008; 295:E1255–1268. [PubMed: 18765679]

Kayo T, Allison DB, Weindruch R, Prolla TA. Influences of aging and caloric restriction on the transcriptional profile of skeletal muscle from rhesus monkeys. Proc Natl Acad Sci U S A. 2001; 98:5093–5098. [PubMed: 11309484]

Kume S, Uzu T, Horiike K, Chin-Kanasaki M, Isshiki K, Araki S, Sugimoto T, Haneda M, Kashiwagi A, Koya D. Calorie restriction enhances cell adaptation to hypoxia through Sirt1-dependent mitochondrial autophagy in mouse aged kidney. J Clin Invest. 2010; 120:1043–1055. [PubMed: 20335657]

Lambert AJ, Merry BJ. Effect of caloric restriction on mitochondrial reactive oxygen species production and bioenergetics: reversal by insulin. Am J Physiol Regul Integr Comp Physiol. 2004; 286:R71–79. [PubMed: 12969875]

Lanza IR, Nair KS. Functional assessment of isolated mitochondria in vitro. Methods Enzymol. 2009; 457:349–372. [PubMed: 19426878]

Lanza IR, Short DK, Short KR, Raghavakaimal S, Basu R, Joyner MJ, McConnell JP, Nair KS. Endurance exercise as a countermeasure for aging. Diabetes. 2008; 57:2933–2942. [PubMed: 18716044]

Lewis SE, Goldspink DF, Phillips JG, Merry BJ, Holehan AM. The effects of aging and chronic dietary restriction on whole body growth and protein turnover in the rat. Exp Gerontol. 1985; 20:253–263. [PubMed: 2419151]

Lin SJ, Kaeberlein M, Andalis AA, Sturtz LA, Defossez PA, Culotta VC, Fink GR, Guarente L. Calorie restriction extends Saccharomyces cerevisiae lifespan by increasing respiration. Nature. 2002; 418:344–348. [PubMed: 12124627]

Lopez-Lluch G, Hunt N, Jones B, Zhu M, Jamieson H, Hilmer S, Cascajo MV, Allard J, Ingram DK, Navas P, et al. Calorie restriction induces mitochondrial biogenesis and bioenergetic efficiency. Proc Natl Acad Sci U S A. 2006; 103:1768–1773. [PubMed: 16446459]

Luhtala TA, Roecker EB, Pugh T, Feuers RJ, Weindruch R. Dietary restriction attenuates age-related increases in rat skeletal muscle antioxidant enzyme activities. J Gerontol. 1994; 49:B231–238. [PubMed: 8056935]

Ma ZQ, Dasari S, Chambers MC, Litton MD, Sobecki SM, Zimmerman LJ, Halvey PJ, Schilling B, Drake PM, Gibson BW, et al. IDPicker 2.0: Improved protein assembly with high discrimination peptide identification filtering. J Proteome Res. 2009; 8:3872–3881. [PubMed: 19522537]

Merry BJ, Holehan AM, Lewis SE, Goldspink DF. The effects of ageing and chronic dietary restriction on in vivo hepatic protein synthesis in the rat. Mech Ageing Dev. 1987; 39:189–199. [PubMed: 2442570]

Michikawa Y, Mazzucchelli F, Bresolin N, Scarlato G, Attardi G. Aging-dependent large accumulation of point mutations in the human mtDNA control region for replication. Science. 1999; 286:774–779. [PubMed: 10531063]

Miller BF, Robinson MM, Bruss MD, Hellerstein M, Hamilton KL. A comprehensive assessment of mitochondrial protein synthesis and cellular proliferation with age and caloric restriction. Aging Cell. 2011; 11:150–161. [PubMed: 22081942]

Mootha VK, Bunkenborg J, Olsen JV, Hjerrild M, Wisniewski JR, Stahl E, Bolouri MS, Ray HN, Sihag S, Kamal M, et al. Integrated analysis of protein composition, tissue diversity, and gene regulation in mouse mitochondria. Cell. 2003; 115:629–640. [PubMed: 14651853]

Morselli E, Maiuri MC, Markaki M, Megalou E, Pasparaki A, Palikaras K, Criollo A, Galluzzi L, Malik SA, Vitale I, et al. Caloric restriction and resveratrol promote longevity through the Sirtuin-1-dependent induction of autophagy. Cell Death Dis. 2010; 1:e10. [PubMed: 21364612]

Nair KS, Halliday D, Ford GC, Garrow JS. Effect of triiodothyronine on leucine kinetics, metabolic rate, glucose concentration and insulin secretion rate during two weeks of fasting in obese women. Int J Obes. 1989; 13:487–496. [PubMed: 2676876]

Nisoli E, Tonello C, Cardile A, Cozzi V, Bracale R, Tedesco L, Falcone S, Valerio A, Cantoni O, Clementi E, et al. Calorie restriction promotes mitochondrial biogenesis by inducing the expression of eNOS. Science. 2005; 310:314–317. [PubMed: 16224023]

Picard M, Ritchie D, Wright KJ, Romestaing C, Thomas MM, Rowan SL, Taivassalo T, Hepple RT. Mitochondrial functional impairment with aging is exaggerated in isolated mitochondria compared to permeabilized myofibers. Aging Cell. 2010; 9:1032–1046. [PubMed: 20849523]

Short KR, Bigelow ML, Kahl J, Singh R, Coenen-Schimke J, Raghavakaimal S, Nair KS. Decline in skeletal muscle mitochondrial function with aging in humans. Proc Natl Acad Sci U S A. 2005; 102:5618–5623. [PubMed: 15800038]

Sohal RS, Ku HH, Agarwal S, Forster MJ, Lal H. Oxidative damage, mitochondrial oxidant generation and antioxidant defenses during aging and in response to food restriction in the mouse. Mech Ageing Dev. 1994; 74:121–133. [PubMed: 7934203]

Sohal RS, Weindruch R. Oxidative stress, caloric restriction, and aging. Science. 1996; 273:59–63. [PubMed: 8658196]

Sreekumar R, Unnikrishnan J, Fu A, Nygren J, Short KR, Schimke J, Barazzoni R, Nair KS. Effects of caloric restriction on mitochondrial function and gene transcripts in rat muscle. Am J Physiol Endocrinol Metab. 2002; 283:E38–43. [PubMed: 12067840]

Tabb DL, Fernando CG, Chambers MC. MyriMatch: highly accurate tandem mass spectral peptide identification by multivariate hypergeometric analysis. J Proteome Res. 2007; 6:654–661. [PubMed: 17269722]

Tabb DL, Ma ZQ, Martin DB, Ham AJ, Chambers MC. DirecTag: accurate sequence tags from peptide MS/MS through statistical scoring. J Proteome Res. 2008; 7:3838–3846. [PubMed: 18630943]

Walther DM, Mann M. Accurate quantification of more than 4000 mouse tissue proteins reveals minimal proteome changes during aging. Mol Cell Proteomics. 2011; 10:M110 004523. [PubMed: 21048193]

Weindruch R, Kayo T, Lee CK, Prolla TA. Microarray profiling of gene expression in aging and its alteration by caloric restriction in mice. J Nutr. 2001; 131:918S–923S. [PubMed: 11238786]

Weindruch, W.; Walford, RL. The retardation of aging and diseases by dietary restriction. Springfield, IL: Charles C. Thomas; 1998.

Wohlgemuth SE, Julian D, Akin DE, Fried J, Toscano K, Leeuwenburgh C, Dunn WA Jr. Autophagy in the heart and liver during normal aging and calorie restriction. Rejuvenation Res. 2007; 10:281–292. [PubMed: 17665967]

Zangarelli A, Chanseaume E, Morio B, Brugere C, Mosoni L, Rousset P, Giraudet C, Patrac V, Gachon P, Boirie Y, et al. Synergistic effects of caloric restriction with maintained protein intake on skeletal muscle performance in 21-month-old rats: a mitochondria-mediated pathway. FASEB J. 2006; 20:2439–2450. [PubMed: 17142793]

Zid BM, Rogers AN, Katewa SD, Vargas MA, Kolipinski MC, Lu TA, Benzer S, Kapahi P. 4E-BP extends lifespan upon dietary restriction by enhancing mitochondrial activity in Drosophila. Cell. 2009; 139:149–160. [PubMed: 19804760]

Highlights

- Caloric restriction preserves mitochondrial function in aging skeletal muscle
- Mitochondrial biogenesis is not increased by caloric restriction
- Caloric restriction maintains integrity of DNA and the proteome

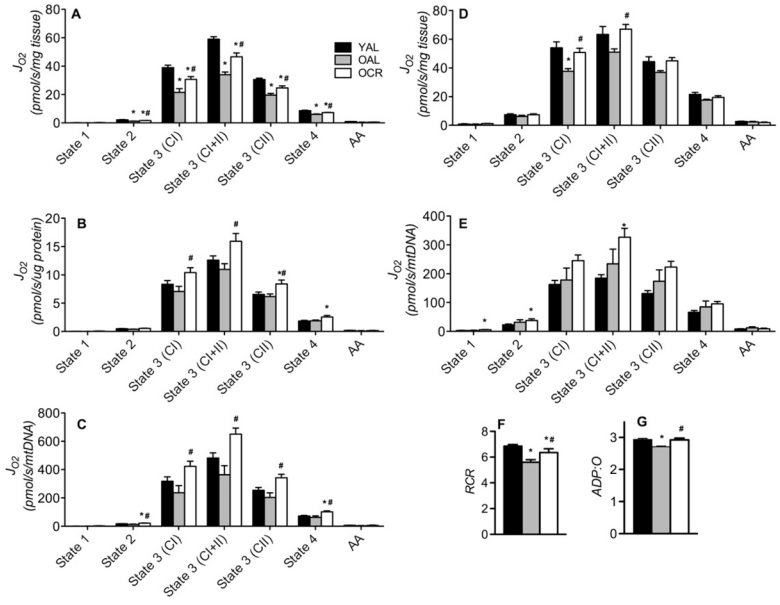

Figure 1. Lifelong caloric restriction prevents age-related reduction in mitochondrial function in skeletal muscle

Respiration rates were measured in isolated mitochondria (A,B,C) and permeabilized fibers (D and E) with substrates targeting complex I (CI), complex I+II (CI+II), and complex II (CII). Non-mitochondrial oxygen consumption was measured in the presence of antimycin A (AA). In isolated mitochondria, respiration rates were expressed per tissue wet (A), mitochondrial protein content (B), and mitochondrial DNA copy number (C). In permeabilized muscle fibers, respiration rates were expressed per tissue wet (D) and mitochondrial DNA copy number (E).

(F and G) Respiratory control ratio (RCR, state 3/state 4) and phosphorylation efficiency (ADP:O) were measured in isolated mitochondria.

Bars represent means ± SEM for young ad libitum mice (YAL), old ad libitum mice (OAL), and old caloric restricted mice (OCR). * represents significant statistical differences from YAL ($P<0.05$, Tukey's HSD). # represents significant statistical differences from OAL ($P<0.05$, Tukey's HSD). N=6–8 per group.

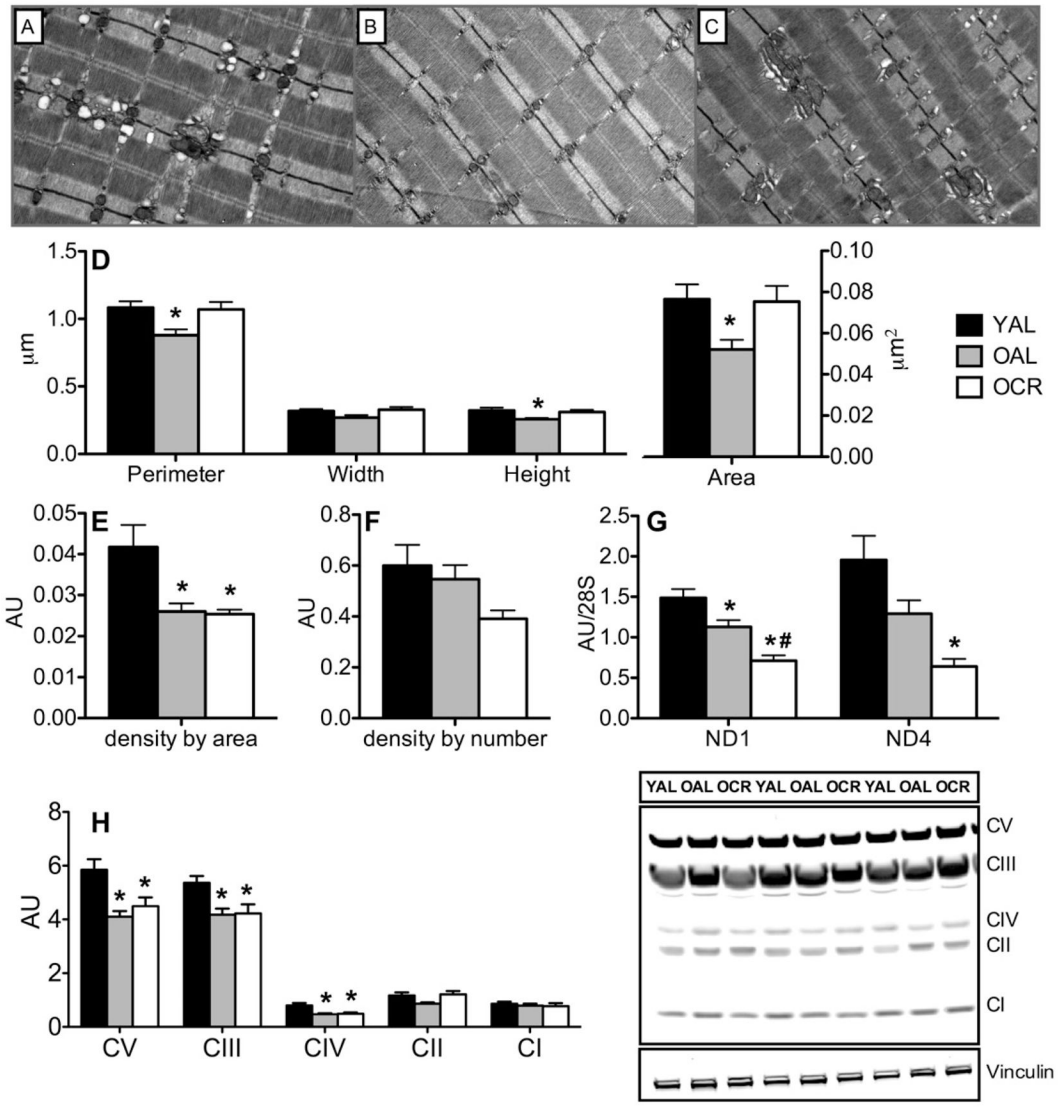

Figure 2. Caloric restriction does not attenuate the reduction in skeletal muscle mitochondrial abundance with aging

(A,B,C) Representative transmission electron micrographs (25,000 × magnification) of skeletal muscle from YAL (A), OAL (B), and OCR (C) mice.

(D) Average perimeter, width, height, and area of mitochondria were measured from digitized images (N=7–8 per group).

(E and F) Mitochondrial density by area and density by number were determined from digitized electron micrographs (N=7–8 per group).

(G) Mitochondrial DNA abundance was measured by rt-PCR using mitochondrial-encoded NADH dehydrogenase subunits 1 (ND1) and 4 (ND4), expressed relative to 28S as a nuclear housekeeping gene (N=10–12 per group).

(H) Respiratory chain protein expression was measured by immunoblot in skeletal muscle lysates and normalized to vinculin as a loading control.

Bars represent means ± SEM for young ad libitum mice (YAL), old ad libitum mice (OAL), and old caloric restricted mice (OCR). * represents significant statistical differences from YAL ($P<0.05$, Tukey's HSD). # represents significant statistical differences from OAL ($P<0.05$, Tukey's HSD). See also figure S1

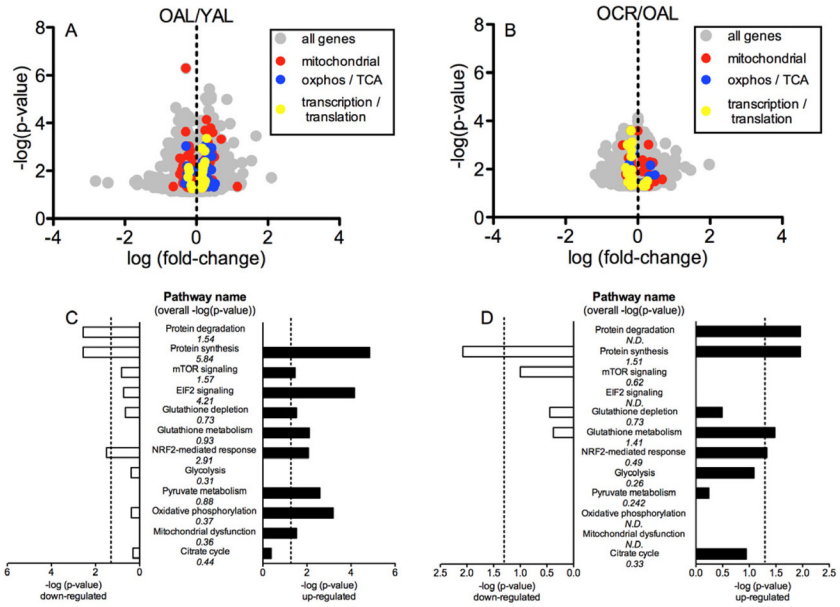

Figure 3. Whole-genome profiling reveals no transcriptional evidence of increased mitochondrial biogenesis with caloric restriction

(A and B) Volcano plots of genes that were found to be differentially expressed in OAL vs. YAL (A) and OCR vs. OAL (B), measured by microarray.

(C and D) Canonical pathways related to mitochondrial energy metabolism, protein turnover, and oxidative stress were assessed from gene expression patterns using Ingenuity Pathway Analysis (IPA). P-values under the pathway name are presented as their −log10 derivatives and were derived using both up-and down-regulated genes involved in each pathway. Histogram bars represent −log10 P-values for each pathway using either exclusively up-regulated genes (black bars) or exclusively down-regulated genes (white bars). Dotted vertical lines represent the threshold for statistical significance ($P<0.05$, $-\log(\text{P-value}) > 1.301$). See also Tables S2, S3, S4, S5, S6, S7.

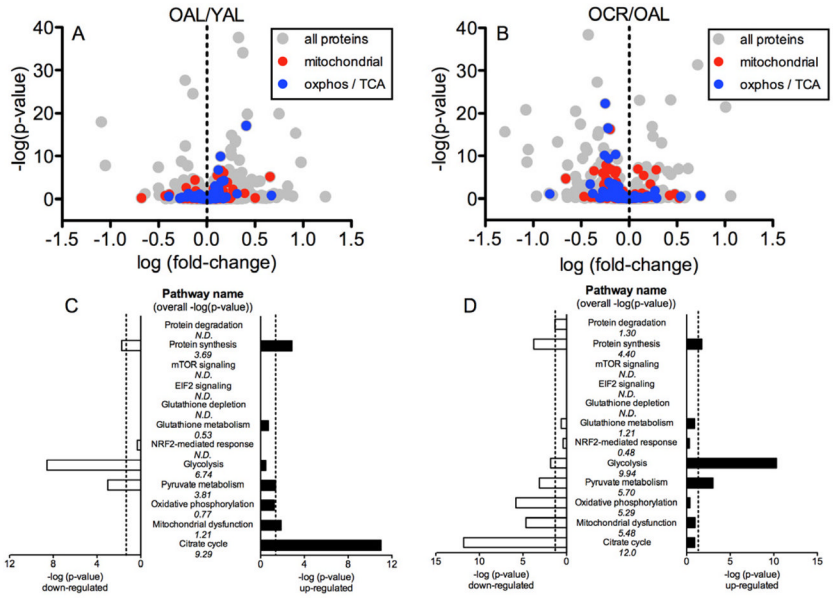

Figure 4. Quantitative proteomics by SILAC mouse reveals decreased expression of mitochondrial proteins with caloric restriction

(A and B) Volcano plots of proteins that were differentially expressed in OAL vs. YAL (A) and OCR vs. OAL (B), measured by using SILAC mouse tissues and mass spectrometry. (C and D) Canonical pathways related to mitochondrial energy metabolism, protein turnover, and oxidative stress were assessed from protein expression patterns using Ingenuity Pathway Analysis. P-values under the pathway name were derived using both up-and down-regulated proteins involved in each pathway. Histogram bars represent P-values for each pathway using either exclusively up-regulated proteins (black bars) or exclusively down-regulated proteins (white bars). Dotted vertical lines represent the threshold for statistical significance ($P<0.05$, $-\log(\text{P-value}) > 1.301$). See also Tables S8, S9, S10, S11, S12, S13.

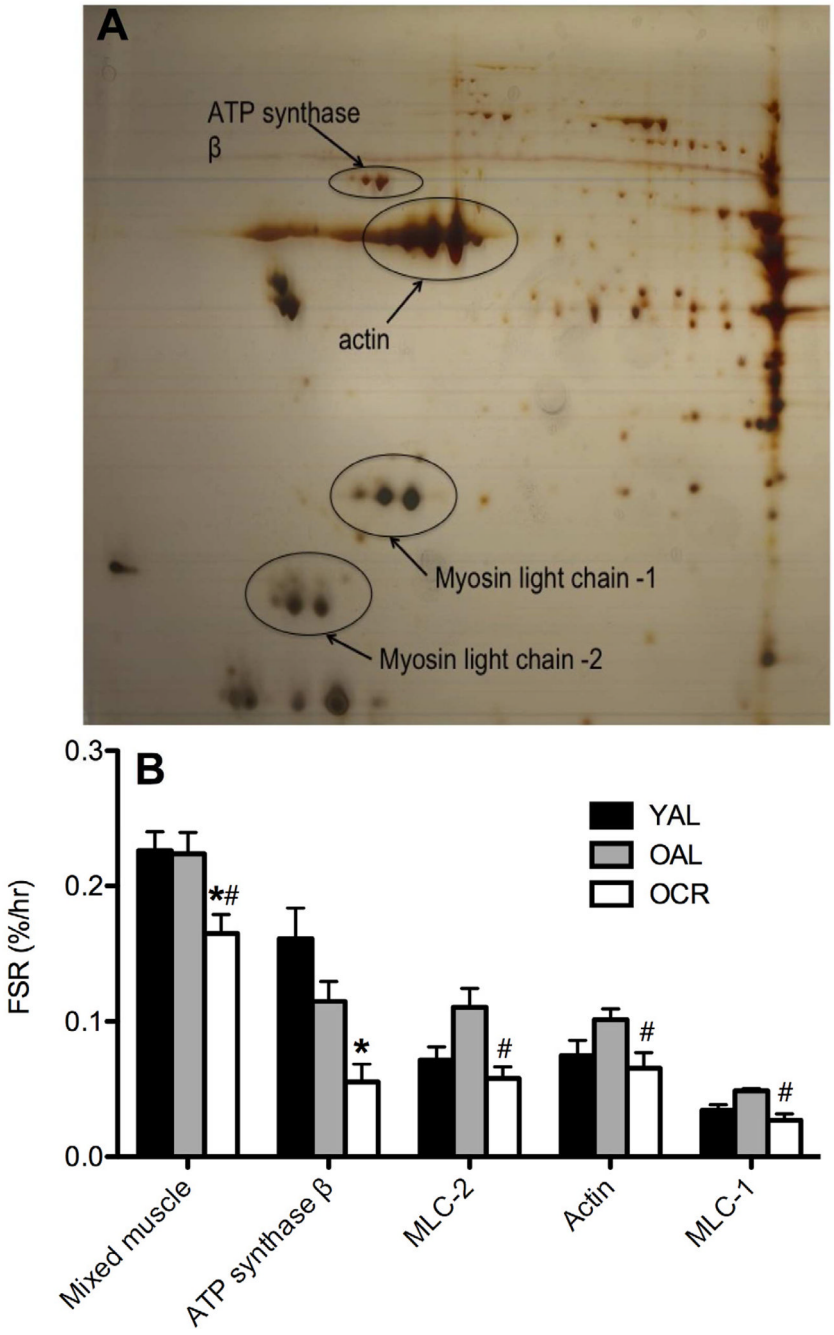

Figure 5. Caloric restriction decreases whole-muscle protein synthesis and fractional synthesis rates of individual proteins

(A) Representative silver-stained 2D gel separation of individual skeletal muscle proteins. (B) Fractional synthesis rates of whole tissue (mixed muscle) and individual skeletal muscle proteins measured by in vivo labeling by intravenous injection of $^{13}C_6$ phenylalanine and mass spectrometry. MLC-1 is myosin light chain 1. MLC-2 is myosin light chain 2. Bars represent means ± SEM for young ad libitum mice (YAL), old ad libitum mice (OAL), and old caloric restricted mice (OCR). * represents significant statistical differences from YAL ($P<0.05$, Tukey's HSD). # represents significant statistical differences from OAL ($P<0.05$, Tukey's HSD). (N=5–8 per group).

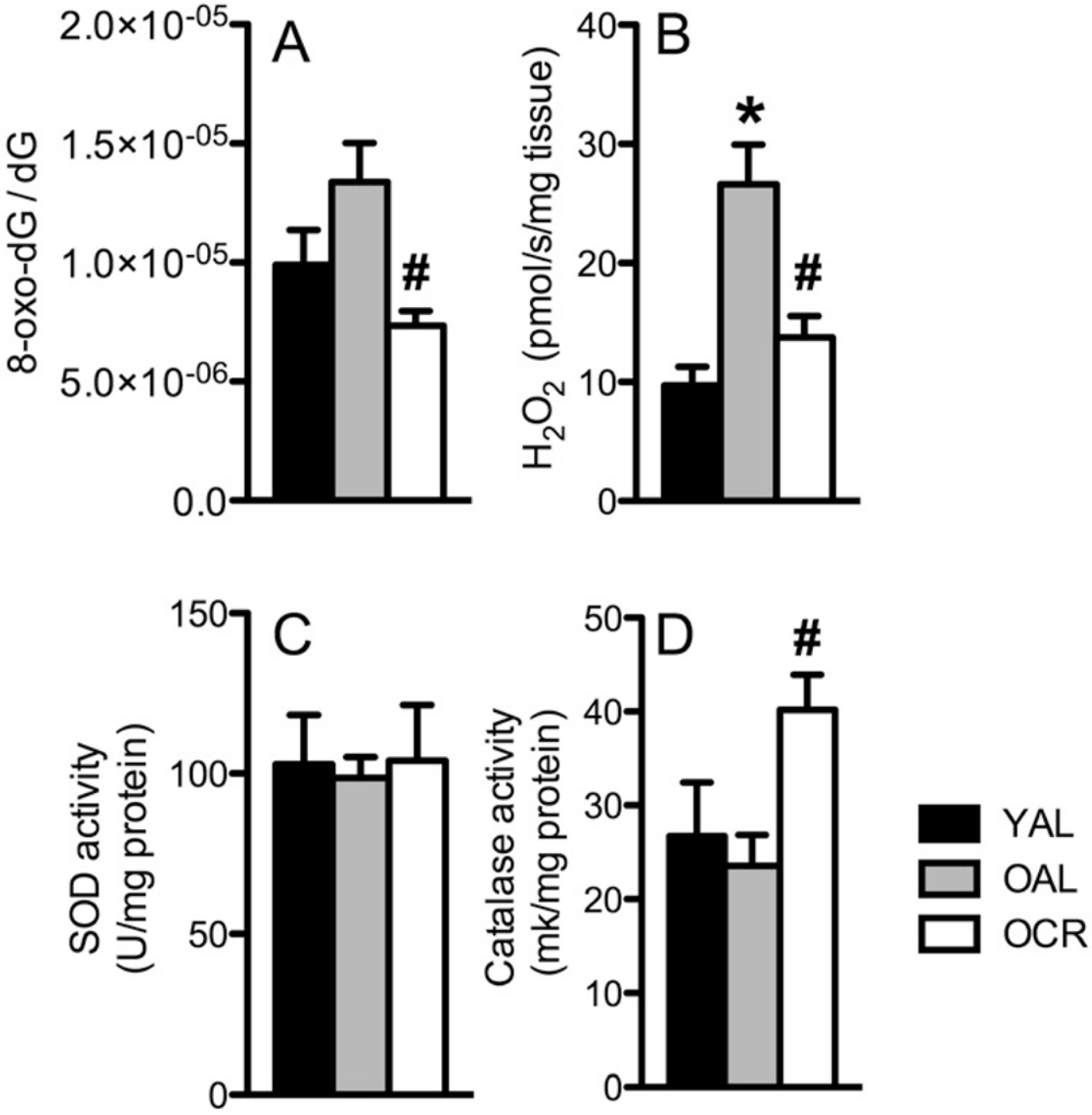

Figure 6. Caloric restriction decreases cellular oxidative damage decreases mitochondrial oxidant emission, and increases antioxidant defenses

(A) Skeletal muscle oxidative damage was determined from 8-Oxo-2′-deoxyguanosine (8-oxo-dG); a major product of DNA oxidation measured by mass spectrometry (N=10–12 per group).

(B) Hydrogen peroxide (H_2O_2) emission was measured in permeabilized muscle fibers by spectrofluorometry.

(C) Maximal activities of superoxide dismutase (D) and catalase were measured by spectrophotometric methods in skeletal muscle homogenates. Bars represent means ± SEM for young ad libitum mice (YAL), old ad libitum mice (OAL), and old caloric restricted

mice (OCR). * represents significant statistical differences from YAL ($P<0.05$, Tukey's HSD). # represents significant statistical differences from OAL ($P<0.05$, Tukey's HSD). (N=5–9 per group)

Table 1

Posttranslational modifications are less abundant with caloric restriction

Blind detection of posttranslational modifications (PTMs) was performed using mass spectrometry in muscle tissues (N=3 per group). The top panel of table 1 lists all detected PTMs supported by at least two unique peptide identifications and twenty peptide-spectrum matches. Accurate precursor masses and fragment ion matches were utilized to attest deamidated peptides. To compare PTM abundance across groups, spectral counts for oxidation and deamidation were normalized and scaled, and compared in a pair-wise fashion using Chi-square test p-values (bottom).

			Spectral Counts		
Mass	**Residues**	**UniMod Annotation**	**YAL**	**OAL**	**OCR**
16	M,F,H,W	Oxidation	1631	1623	1447
1	N,Q	Deamidation	1312	1474	1289
42	N-terminus	Acetylation	1325	1382	1367
32	M,W	Dioxidation	388	331	337
89	C	*Unexpected*	264	254	298
14	E,H,K	Methyl	248	259	245
48	C	Cysteic acid or Selenium	160	174	130
−46	M	*Unexpected*	96	84	92
28	K	Dimethylation or formylation	92	90	74
34	H,K,M	*Unexpected*	86	89	80
−48	M	Loss of Methyl Side Chain	61	57	65
43	M	Carbamylation	40	56	46
162	W	Hexose	27	28	27
192	W	*Unexpected*	21	27	33
4	W	Kynurenin	17	25	20
121	W	*Unexpected*	28	15	16
73	C	*Unexpected*	8	18	6
89	W	*Unexpected*	6	12	8

	Spectral Counts[a]			Differential Expression P-value[b]		
PTM	**YAL**	**OAL**	**OCR**	**OAL vs. YAL**	**OAL vs. OCR**	**OCR vs. YAL**
Oxidation M,W,F,H	1001	996	888	0.4125	0.0464	0.0053
Deamidation N,Q	805	905	791	0.0211	0.0172	0.9319